Thermal conductivity of pure or iron-doped $YBa_2Cu_3O_{7-\delta}$ with or without an excess of CuO

1994 J. Phys.: Condens. Matter 6 6305

(http://iopscience.iop.org/0953-8984/6/31/030)

J. Phys.: Condens Matter 6 (1994) 6305–6316. Printed in the UK

Thermal conductivity of pure or iron-doped $YBa_2Cu_3O_{7-\delta}$ with or without an excess of CuO

M Houssa†, H Bougrine†, M Ausloos†, I Grandjean‡ and M Mehbod‡
† SUPRAS, Université de Liège, Institut de Physique B5, B-4000 Liège, Belgium
‡ Service de Physique des Solides, Université Libre de Bruxelles, CP 233, Boulevard du Triomphe, B-1050 Brussels, Belgium

Received 24 January 1994, in final form 21 April 1994

Abstract. The thermal conductivities of $YBa_2(Cu_{1-x}Fe_x)_3O_{7-\delta}$ + y% CuO ceramics for $0 < x < 0.03$ and $0 < y < 5$ have been measured. The thermal conductivities of all samples exhibit a minimum in the vicinity of the critical temperature T_c and a maximum near $T_c/2$. These results are interpreted with the help of an electronic model, i.e. supposing that the main contribution to the thermal conductivity below T_c is due to electron scattering in the CuO_2 planes. Within a simple two-fluid model derived from kinetic theory, taking into account the temperature dependence of the electronic relaxation time and the normal charge carrier concentration, we obtain theoretical curves which reproduce the experimental results quite well. We also take into account the porosity of the samples (in term of an intergrain contribution) to derive the electronic thermal conductivity. The parameter values of the model and the observed minimum are explained in terms of physical properties. In particular, the contribution of superconductivity fluctuations to the thermal conductivity is shown to be negligible with respect to other mechanisms.

1. Introduction

The thermal conductivities of high-critical-current-density (J_c) superconductors (HJSs) such as $YBa_2Cu_3O_{7-\delta}$ (YBCO) have been investigated theoretically [1–9] and experimentally [10–14] in several publications so far; only those which pertain to investigations in the temperature range encompassing the critical temperature are quoted here. Yet, few experimental results concerning thermal conductivity in *doped* YBCO have been published [14]. We discuss here the thermal conductivities of pure and specifically doped YBCO compounds from 30 to 200 K. In contrast with the situation in other superconductor ceramics [1, 2], we observe that κ decreases as the temperature is lowered below T_c, presenting an unusual minimum in the proximity of T_c and then increases to reach a maximum near $T_c/2$. We interpret these results with the help of the electronic model of thermal conductivity [5, 8, 15], taking into account explicitly the temperature dependence of the charge carrier concentration and the electronic relaxation time in the same framework as used by Delap and Bernhoeft [6].

According to this interpretation [5, 8, 15], the main contribution to the thermal conductivity structure below T_c is due to normal charge carriers, the sign of which is to be determined from for example Hall and Seebeck coefficients values, or from band-structure calculations. Indeed, below T_c, since charge carriers condensing into Cooper pairs carry no heat, the thermal conductivity is thus ensured by normal charge carriers. Since the normal charge carrier scattering rate in HJSs has been observed to decrease rapidly below T_c [16, 17], κ should *increase* in the superconducting state.

0953-8984/94/316305+12$19.50

Much work has been done on untwinned single crystals [5, 15]. However, if the sample presents structural defects or impurities, free charge carriers are scattered by these defects and κ should *decrease*. Therefore, this 'competition' between the increase in κ due to the increase in the mean free path of normal charge carriers (related to the superconducting transition) and the decrease in κ due to the presence of defects can lead to a minimum in the temperature dependence of the thermal conductivity.

In choosing Fe as an impurity we also modify the characteristic grain size basic dimension [18] besides reducing the critical temperature. This has much relevance in the presence of a magnetic field [14] since there is then competition between the characteristic lengths, i.e. the coherence length, the penetration depth, and the typical grain and defect sizes.

Introducing CuO as a 'coating impurity' should also lead to a modification of the mean free path (even in the absence of a field) but without altering the critical temperature. The combination of both 'impurities' is also of interest in order to observe the gradual variation in properties between pure or iron-doped samples with and without excess of CuO. It is expected on the one hand that Fe is then partially removed from the Fe–YBCO tweeded grains, consequently modifying T_c, the mean free path and the intergrain contribution. It is of great interest to provide a theory which can encompass these varied situations.

2. Experimental results

The samples of YBCO ceramics are pure or contain 3% Fe and 5% CuO, respectively, or both. The samples are all prepared by solid state reactions in the same conditions. The raw materials Y_2O_3, CuO, $BaCO_3$ and Fe_2O_3 are mixed in an agate mortar for 1 h. The samples are then calcined at 930 °C for 12 h, reground, sintered at 940 °C for 12 h, reground and sintered again at 920 °C for 12 h. For each process, the decrease in temperature lasts 30 h in an oxygen atmosphere.

After each thermal cycle, the samples are characterized by various structural, electrical and magnetic analyses [19]. X-ray analyses and scanning electron microscopy show that Fe atoms are substituted into the superconducting grains, where excess of CuO forms secondary phases. The AC magnetic susceptibility measurements have then been performed in order to estimate the critical temperature $T_c^{(M)}$ of the samples (table 1).

Various concentrations of Fe impurities and excess of CuO have been examined. We report here only four cases taken from pellets of about 110 mm^3 (15 mm × 3 mm × 2.5 mm) original size with the following symbols, abbreviations and nominal formulae:

Samples 1, YBCO≡$YBa_2Cu_3O_{7-x}$, open circles;

Samples 2, YBCO+3% Fe≡$YBa_2(Cu_{0.97}Fe_{0.03})_3O_{7-x}$, full circles;

Samples 3, YBCO+5% CuO≡$YBa_2Cu_3O_{7-y'}$ + 5% CuO, open triangles;

Samples 4, YBCO+3% Fe+5% CuO≡$YBa_2(Cu_{0.97}Fe_{0.03})_3O_{7-y''}$ + 5% CuO, open diamonds.

No secondary phase except CuO has been found in samples 3 and 4. The Fe-doped samples have been much studied elsewhere [14, 18] and found to be homogeneous.

The critical temperatures of these cuprates (see table 1) have been estimated by considering the sharp transition in the thermoelectric power (TEP) at $T_c^{(S)}$ defined at the inflection point (which is very close to the temperature at which the TEP vanishes) [20] and corresponds to the superconductivity onset as measured by susceptibility [19]. It should be noted, however, that the critical temperatures $T_c^{(M)}$ and $T_c^{(S)}$ determined from such different

Table 1. Values of the parameters for the fit (see text) to the experimental data (figures 1, 2 and 5): $T_c^{(M)}$ and $T_c^{(S)}$ are the critical temperatures measured via magnetic susceptibility measurements [19] and the thermopower measurements [20], respectively; μ and ν are the parameters related to the phonon umklapp processes in equation (1): κ_e^n is the normal state electronic part of κ in equation (4); χ is the ratio of the zero-gap energy $\Delta(0)$ to T_c in equation (8); α and β are parameters related to the magnitude of the electronic relaxation time; ζ is the critical exponent of the fluctuation-like term in the relaxation time in equation (9).

Sample	Nominal composition	$T_c^{(M)}$ (K)	$T_c^{(S)}$ (K)	μ (W m^{-1} K^{-1})	ν	κ_e^n (W m^{-1} K^{-1})	χ	α (10^{-14} s)	β (10^{-12} s)	ζ
1	Pure YBCO	91	91	1.84	0.38	0.9	1.5	1.32	22	6
2	YBCO+3% Fe	76	77	1.27	0.32	0.7	1.2	0.36	4.9	4
3	YBCO+5% CuO	91	91	0.70	0.09	1.2	0.6	1.94	1.5	4
4	YBCO+3% Fe+5% CuO	80	84	0.86	0.26	0.5	3.0	1.27	210	8

properties are almost the same. They do not differ for pure and CuO–YBCO samples but differ by at most 4 K for the Fe– and Fe+CuO-'doped' samples (see table 1). Note also that the nature of the charge carriers (electrons or holes) is determined via the sign of the TEP [20]. However, the type of charge carrier does not have much relevance here because equations related to the thermal conductivity do not contain the sign of the charge carriers.

The shift in T_c between the pure YBCO and the Fe-doped samples and samples with an excess of CuO is consistent with literature data [21,22]. The shift is of the order of 10–15 K for 3% Fe with respect to the CuO content. It is remarkable that the Fe-doped samples with extra CuO present a higher T_c. This is probably due to the 'absorption' of Fe by CuO inclusions which depopulate doped YBCO grains from the substituted Fe-doped grains.

The thermal conductivities of these samples have been measured using a precise and sensitive simultaneous method [23]. We have developed the instrumentation using a steady-state method over the range 4.2–300 K and we have chosen the 'longitudinal heat flow' method. The temperature gradient on the samples was about 2.5 K cm^{-1}. The technique is briefly described in the appendix. The resulting data are shown in figure 1. We observe that the value of κ at its peak, i.e. $\kappa(T_c/2)$, decreases from about 13 to 4 W m^{-1} K as the samples are doped with Fe and with excess CuO or both. These 'impurities' thus act as *extra scattering* centres in YBCO grains but also at *intergrain boundaries*. The thermal conductivity of these samples exhibits a minimum near 80–82 K except for the sample containing some excess CuO only (see figure 1, open triangles) which presents a small minimum above the critical temperature, near 95 K. Note that the critical temperature transition is (*a posteriori*) marked by a break which occurs in the slope of $\kappa(T)$. In the normal state, the thermal conductivity presents a smooth decay sometimes with some structure (pure, Fe-doped and Fe+CuO-doped samples) near 120 K, in contrast with the CuO–YBCO composite sample for which κ smoothly increases above T_c.

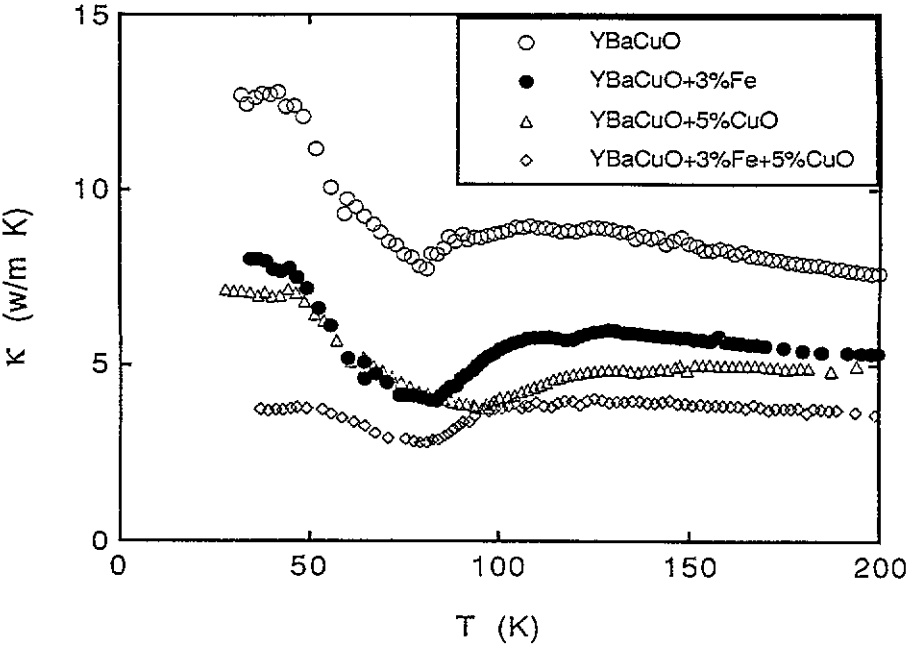

Figure 1. Thermal conductivity of different pure or doped YBCO ceramics versus temperature.

3. Theoretical analysis

We follow the idea that the contribution to the thermal conductivity in such well oxygenated YBCO can be separated into a phonon term κ_p and an electronic term κ_e; the main structure is, however, thought to arise from an electronic origin [5, 8, 15]. In order to derive the electronic contribution to the thermal conductivity of these samples, we use the following method. First, we fit the normal-state thermal conductivity above T_c up to $2T_c$ with an expression for the phonon contribution κ_p, supposed to originate in umklapp processes [24]:

$$\kappa_p^n = \mu \left(\frac{T_D}{T}\right)^{\nu} \tag{1}$$

where T_D is the Debye temperature of the order of 300 K [25] and is therefore fixed at that value here.

In order to take into account the granularity of the samples, we also consider the contribution κ_{gb} from grain boundaries (intergrain contribution) to the thermal conductivity. According to the percolation model [26], the latter contribution is given by

$$\kappa_{gb} = \kappa F \left(\frac{Q - Q_c}{1 - Q_c}\right)^t \tag{2}$$

where $Q = 1 - \Pi$ with Π the porosity; Q_c is the percolation threshold, t a critical exponent and F the relative area of the contact spot in sintered samples. The porosity of our samples is estimated to be 10% ($\Pi = 0.1$). Taking $F = 0.75$, $Q_c = 0.12$ and $t = 2$ [26], we obtain $\kappa_{gb} = 0.59\kappa$ leading to an intragrain contribution $\kappa_{ig} = \kappa - \kappa_{gb} = 0.41\kappa$. This intragrain contribution is then supposed to be the sum of an electronic contribution and a phonon contribution:

$$\kappa_{ig} = \kappa_e + \kappa_p. \tag{3}$$

The normal-state electronic thermal conductivity κ_e^n is estimated with the help of the Wiedeman–Franz law (WFL)

$$\kappa_e^n = L_0 \sigma T \tag{4}$$

where $L_0 = 2.44 \times 10^{-8}$ V^2 K^{-2} is the Lorentz number [24] and σ the electrical conductivity which is linear with T^{-1} in the normal state of HJSs. Using electrical conductivity data for these kinds of sample [19] (taking the porosity also into account), we obtain from the WFL a constant κ_e^n lying between 0.5 and 1.2 W m^{-1} K^{-1} (see table 1).

Fits to the data for $T > T_c$ using equations (1)–(4) are shown in figure 2, with μ, ν and κ_e^n-values given in table 1. Note that the ν-values are much smaller than unity.

Then, like Yu *et al* [5, 8], we suppose that κ_p is not much affected by the superconducting transition, assuming that there is no drastic change in the phonon spectrum below T_c. Therefore, the electronic part of the thermal conductivity in the superconducting state is given by

$$\kappa_e^s = \kappa_{ig}^s - \mu \left(\frac{T_D}{T}\right)^{\nu}. \tag{5}$$

Note that the value of κ_e^n given by the WFL (4) affects the magnitude of κ_e^s and not its temperature dependence. Indeed, if the value of κ_e^n is altered, e.g. if the WFL does not truly

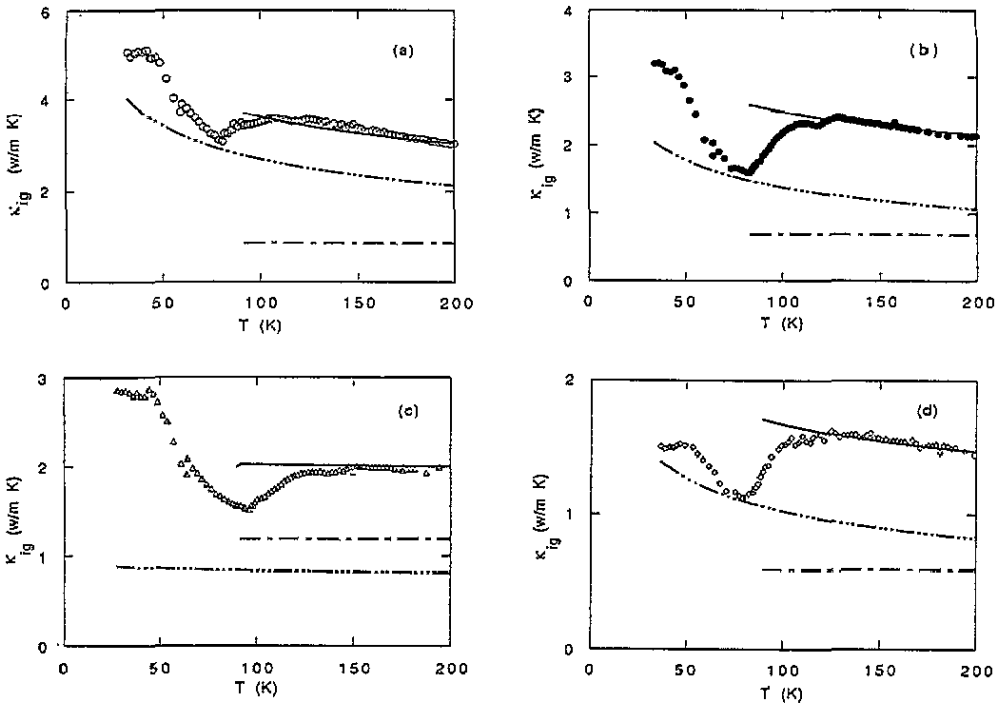

Figure 2. Intragrain contribution to the thermal conductivity versus temperature with the same symbols as in figure 1: — · · · —, derived phonon thermal conductivity κ_p from equation (1); — · —, derived electronic thermal conductivity κ_e^n from the WFL law (equation (4)); ——, sum of the electronic and phonon contributions to the intragrain thermal conductivity (equation (3)). The fitting parameters are given in table 1.

hold, the magnitude of κ_p^n should just be shifted according to equation (3) and consequently to equation (1); this should modify the value of the parameter μ only and not ν. Then, following equation (5), only the magnitude of κ_e^s is also modified.

We have then used a well known formula derived from kinetic theory for the electronic component of the thermal conductivity [27]:

$$\kappa_e = \frac{\pi^2}{3} n_e(T) \frac{k_B^2 T}{m^*} \tau_e(T) \tag{6}$$

where $n_e(T)$ is the concentration of normal charge carriers of effective mass m^* and $\tau_e(T)$ is the temperature-dependent electronic relaxation time.

We consider a two-fluid model in which condensation of charge carriers occurs below T_c, and supposing that charge carriers are fully condensed into Cooper pairs at zero temperature [15, 28]. We write the temperature dependence of normal charge carriers as [29]

$$n_e(T) = n_c \exp\left(\frac{-\Delta(T)}{k_B T}\right) \tag{7}$$

where n_c is the density of charge carriers at the critical temperature, i.e. of the order of 10^{27} electrons m^{-3} [25] and $\Delta(T)$ a temperature-dependent energy gap. We write the temperature dependence of the gap as [29]

$$\Delta(T) = \chi k_B T_c \sqrt{\frac{T_c - T}{T_c}} \tag{8}$$

where $\chi = \Delta(0)/k_B T_c$. The temperature dependence of the normal charge carriers using equations (7) and (8) is shown in figure 3 for different values of the parameter χ.

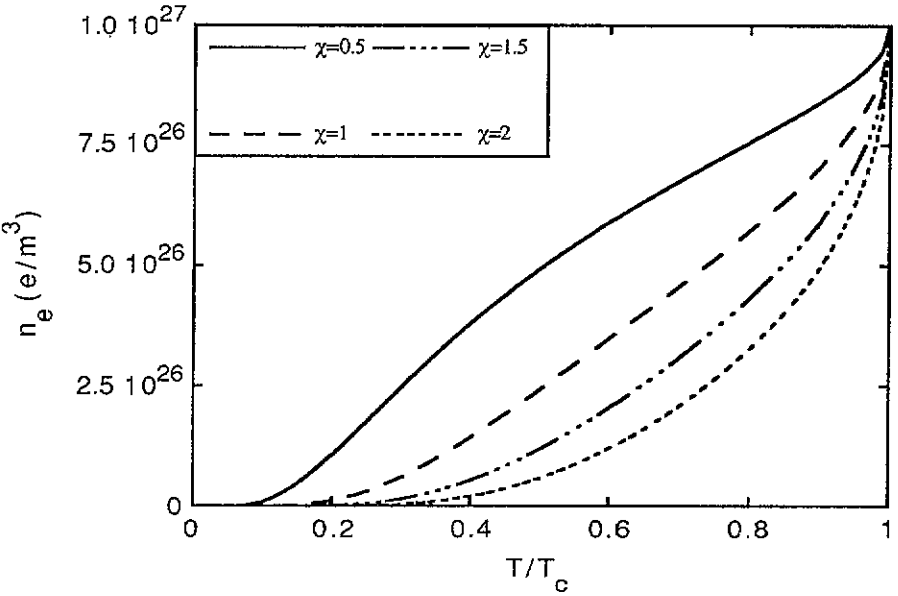

Figure 3. Normal electron density n_e as a function of reduced temperature in the complete condensation model (equations (7) and (8)) for different χ-values. The value of n_c is chosen to be 10^{27} electrons m^{-3}.

The electronic relaxation rate is given by the semi-empirical model of Delap and Bernhoeft [6]:

$$\tau_e(T) = \alpha \left(\frac{T_c}{T}\right)^2 + \beta \left(\frac{T_c - T}{T_c}\right)^{\zeta} \tag{9}$$

where the first term represents the electron–electron relaxation time in a Fermi liquid [30] and the second term takes into account the increase in the relaxation time of normal charge carriers observed in HJSs due to fluctuations [31]. The theoretical behaviour of τ_e is presented in figure 4 for different values of the parameter ζ and the ratio β/α.

Theoretical curves of κ_e^s obtained with the help of the above equations (6)–(9) are shown in figure 5 for the fitting parameters given in table 1, and with $m^* = 4m_0$ (where m_0 is the free-electron mass), $n_c = 3 \times 10^{27}$ electrons m^{-3} and $T_D = 300$ K [25]. Fits to the experimental data below T_c are quite reasonable. The overall shape of the thermal conductivity is well reproduced for such systems with different T_c and doping conditions. The minimum is reproduced and the maximum at $T_c/2$ is obtained.

4. Discussion and conclusion

We have analysed the thermal conductivity of several YBCO ceramics, both pure and doped with Fe or CuO and with both impurities. We have interpreted the behaviour of κ using

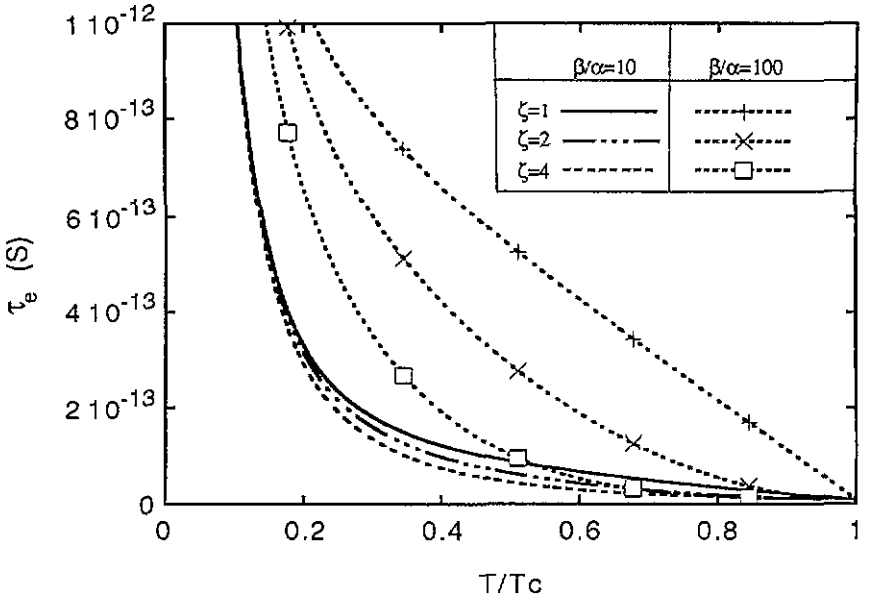

Figure 4. Normal electron relaxation time τ_e as a function of reduced temperature according to equation (9) for different values of the critical exponent ζ and the ratio α/β.

an electronic model taking into account the complete condensation of charge carriers at zero temperature and the rapid rise in the electronic relaxation time below T_c. We have considered an intragrain contribution to κ supposed to be due to electrons and phonons as well as an intergrain contribution arising from grain boundaries. Note that we should have obtained negative values for κ_e^s if we had ignored the latter contribution.

Fits to the data are quite reasonable with a value of the parameter ζ close to 4 (we have imposed the theoretical constraint that ζ be an integer) for the fluctuation-like term in the relaxation time except for the 'dirtiest' sample doped with Fe and containing an excess of CuO in which $\zeta = 8$. These values have to be contrasted with that found ($\zeta = 2$) for an untwinned YBCO single crystal in a previous report [15], indicating that the temperature behaviour of the fluctuation is usually affected by the texture or the granularity of the sample as in electrical resistivity data [31–34]. Hence ζ is a measure of the defect structure of the sample [35].

The values of α and β lead to a relaxation time of the order of 10^{-13} s. Note that the fluctuation contribution to the relaxation time is negligible with respect to the electron–electron scattering mechanism in the vicinity of T_c ($0.8T_c < T < T_c$). Note also that, in this model, τ_e is supposed to increase indefinitely for $T \to 0$. A more exact theory would need to take into account the leveling off of τ_e at low temperatures. It is immediately obvious that κ_e would then decrease towards some residual value consistent with the uncondensed carriers at low temperatures.

χ represents the ratio of the energy gap $\Delta(0)$ at zero temperature to T_c and leads to zero-gap energies lying between 5 and 25 meV comparable with values found from diffusivity measurements ($\Delta(0) \simeq 15$ meV) [36] and infrared spectroscopy measurements ($\Delta(0) \simeq 20$ meV) [37]. The value of ν is quite unusual since the phonon umklapp process should lead to $\nu = 1$. This disagreement with respect to such a classical theoretical value may be due to granularity [38], porosity [39] or impurity effects. Similarly the value of μ has not been theoretically estimated.

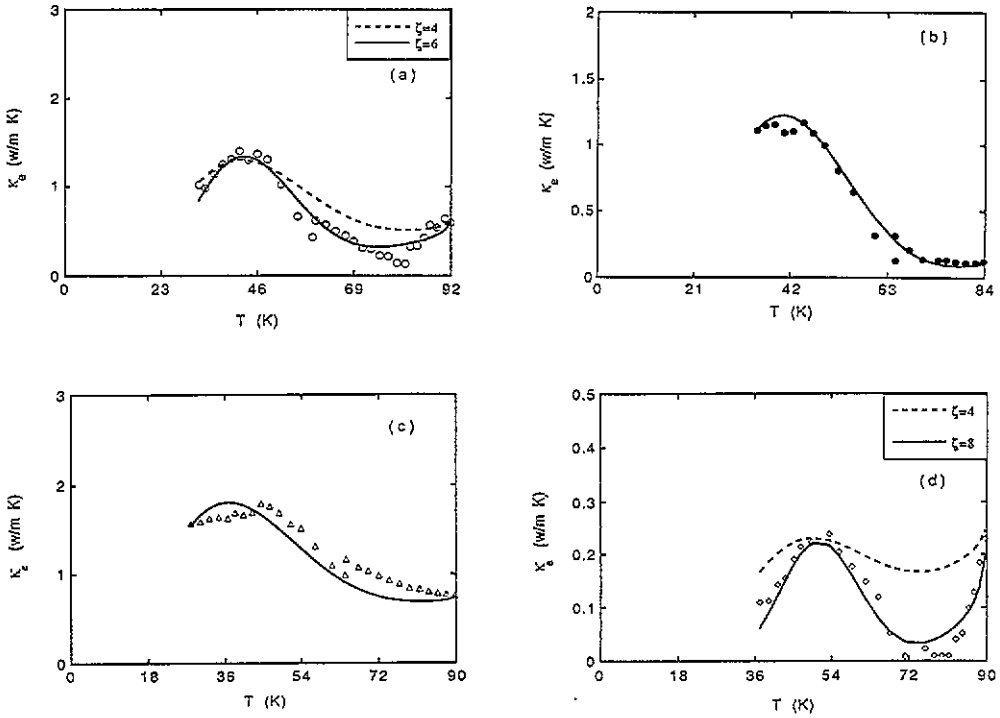

Figure 5. Temperature dependence of κ_e^s and calculated fits taking into account the temperature dependence of the carrier density and the carrier relaxation rate according to equations (6)–(9) for $n_e = 3 \times 10^{27}$ electrons m^{-3}, $m^* = 4m_0$ and $T_D = 300$ K with the same symbols as in figure 1. The best fits (——) are for parameters given in table 1 with correlation factors (*a*) $R = 0.97$, (*b*) $R = 0.99$, (*c*) $R = 0.94$ and (*d*) $R = 0.95$. For the (*a*) and (*d*) cases, the curve $\zeta = 4$ is shown by a broken line.

Finally, it is worth stressing that the minimum in κ near T_c is well reproduced in our theoretical model. From the above, it can be seen that the minimum occurs because of the competition between the charge carrier relaxation time and the temperature variation in the number of carriers. In the case of *inhomogeneous* systems indeed, the Gaussian fluctuations in the order parameter (or $\Delta(T)$) are much damped and occur in a region near T_c where n_e is thus varying greatly (see figure 3 for large χ) in contrast with τ_e which is then quasi-constant. This observation is in full agreement with the fact that in *pure* systems [4, 5] no minimum is seen near T_c. It is thus noted here that the thermal conductivity is an interesting test of the 'cleanness' or 'dirtiness' of superconducting ceramics.

Note that, in the normal state, κ decreases for pure and Fe-doped YBCO (with or without an excess of CuO) while κ increases for the YBCO+5% CuO sample. In fact, above T_c, the temperature dependence of the phonon contribution κ_p is determined by the 'competition' between electron–phonon scattering for which κ increases with increasing temperature [1], and phonon–phonon umklapp scattering for which κ decreases [4]. As the YBCO+5% CuO is a quite well oxygenated system, κ_p may be essentially limited by electron–phonon scattering and κ should then increase above T_c, in agreement with experimental data.

It is in order finally to contrast here the present results with those which should be obtained in the 'phonon model' [40] in which a minimum (but in the form of a break in slope) occurs just at T_c and is thus followed by a *rising* curve *above* T_c. It seems unlikely

that the 'phonon model' could lead to a minimum below T_c (except for strange parameter values).

Acknowledgments

Part of this work has been financially supported through the Impulse Program on High Temperature Superconductors of the Belgium Prime Minister Science Policy Service (SPPS) under contracts SU/02/013 and SU/02/09. We also thank R Deltour for his interest and comments. MH thanks IRSIA (Brussels) for a research fellowship.

Appendix

We have used a highly sensitive method for simultaneously measuring the thermal conductivity and the TEP of solids. The method has been used in several cases [14, 41, 42]. We have thereby proved the sensitivity of the method with respect to losses by radiation and convectivity and ensured that residual temperature and potential differences are taken into account. Thus the 'best conditions' for thermal conductivity measurements are realized. The thermal conductivity has indeed been shown to be highly sensitive to experimental conditions [41, 42], the less so for the TEP [23].

In the present case, we have developed the instrumentation using a steady-state method over the range 4.2–300 K. We have chosen the 'longitudinal heat flow' method [43], in particular searching for an 'absolute' measurement of κ. According to the type of sample which is available (either bars or discs), we can in fact choose between a rod or a plate 'absolute method' [43].

The quasi-steady-state method has been chosen in order to monitor the physical quantities of interest as precisely as possible in the vicinity of a phase transition, in a regime when for example quasi-equilibrium conditions have to be reached [42]. Having rod-like samples, we imposed strict conditions of minimal thermal losses by conduction and radiation. The experimental chamber contains basically two heat sinks and two radiation shields [23]. The vacuum condition was 5×10^{-7} Torr. The radiation shield around the sample and its heater H_1 were controlled by a secondary heater H_0.

The cold sink (CS) temperature is kept constant at a set-point temperature by an electrical heater H_2. The CS temperature T_{CS} is measured with a silicon diode DT-471. The difference between the set point and the CS temperature is then calculated by the temperature controller, and a proportional power is then supplied automatically by this controller in order to re-equilibriate the temperature.

A Pt resistance thermometer is used to measure the temperature of the hot sink (HS), or 'sample holder', in the range 80 K $< T <$ 300 K. Below 80 K, the HS temperature is measured with a carbon–glass (CG) resistor. Both thermometers are glued by Apiezon grease into two holes bored into the HS. Both thermometers were calibrated by Lake Shore Cryotronics. Calibrated copper–constantan (Cu–Ct) thermocouples were used to measure the temperature differences. The wires 15 cm long and 0.08 mm in diameter are thermally anchored at the HS and also where the cold junction of the thermocouples is located. The hot junctions are fixed by electrical discharge on thin pure Cu plaquettes and fixed on the sample by indium soldering. The errors due to the thermal resistance between the sample and the thermocouple are estimated to be 0.02 K.

The DC through and the voltage drop across the sample heater H_1 are measured with great accuracy; the current (usually between 15 and 40 mA) is measured through a calibrated

resistance while the voltage drop is measured by a four-probe method with several current reversals. The error on the supplied power to the sample through this heater is less than 1%.

The temperature difference between the cold end of the sample and a radiation-compensating heater H_0 is measured with a differential Cu–Ct thermocouple. The larger this difference the greater is the heat loss through radiation from the sample. To reduce such a loss, the computer switches on the heater H_0 which is connected to a programmable current source and adjusts the convenient power to bring back the temperature difference to the minimum, i.e. to a few millikelvins.

Note that, to reduce the thermal resistance between the sample and the HS, the sample cold end either is fixed by an indium solder point inside a hole of the HS or is soldered on the HS top (depending on the sample length, be it long or short, respectively).

The hot thermocouple extremities are spot soldered on a thin (about 3 mm^2 in area) Cu plaquette on the sample. The thermocouple positions are not joined of course. Voltage drop wire extremities are soldered on the Cu block HS for which the temperature is maintained by a feedback system through a secondary heater. The wires are wound on the copper block sample holder for thermalization. From the Cu block and extremities, Cu wires lead to precision nanovoltmeters at ambient temperature.

When H_1 is switched off ($Q = 0$), the temperature difference ΔT across the sample should be zero. Unfortunately, in practice, there always remains some finite residual voltage between the wire extremities. This implies a residual temperature difference ΔT_r (T_0), and a residual heat flow in the sample, which is of variable sign [23]. In the data acquisition and subsequent analysis, we do take into account these residual temperature and potential differences on the sample before employing a heat flow.

The thermal run then goes as follows: we stabilize the CS temperature through the regulation H_2. Some heat flows into the sample through the sample holder, thermocouples, heater H_1, surrounding, etc, and introduces some 'residual potential difference' V_i (less than 500 nV). All the 'residual' V_i-values are measured in the steady state. They correspond to some 'residual temperature difference' (less than 0.3 K in this work—a maximum which is reached at room temperature). The temperature difference across the sample is then applied (during a pre-programmed time decided upon at the beginning of the experimental run). This difference varies between 2 and 3 K. After the steady state has been reached, new V_j-values are then measured, and the calculations of T, ΔT and κ are made. For the latter, we use the differential Fourier equation for the thermal conductivity $\kappa(T)$ for a one-dimensional heat flow $Q(T)$ (i.e. the power input from H_1) through a 'linear' sample of length L (and section S) measured *between* the thermocouples in a thermal difference $\Delta T(T)$, i.e. we use the steady-state solution

$$\frac{Q(T)}{S} = \kappa(T)\frac{\Delta T(T)}{L} \tag{A1}$$

where the value of $\Delta T(T)$ is measured taking into account the thermocouple voltage values at the appropriate temperatures.

References

[1] Uher C 1990 *J. Supercond.* 3 337 and references therein

[2] Jezowski A and Klamut J 1990 *Studies of High Temperature Superconductors* ed A Narlikar (Singapore: Nova Science) and references therein

[3] Richardson R A, Peacor S D, Nori F and Uher C 1991 *Phys. Rev. Lett.* **67** 3856
[4] Peacor S D, Richardson R A, Nori F and Uher C 1991 *Phys. Rev.* B **44** 9508
[5] Yu R C, Salamon M B, Lu J P and Lee W C 1992 *Phys. Rev. Lett.* **69** 1431
[6] Delap M R and Bernhoeft N R 1992 *Physica* C **195** 301
[7] Wermbter S and Terwordt L 1992 *Physica* C **196** 383
[8] Yu R C, Salamon M B and Lu J P 1993 *Phys. Rev. Lett.* **71** 1658
[9] Williams W S 1993 *Solid State Commun.* **87** 355
[10] Sera M, Shamoto S and Sato M 1991 *Physica* C **185–9** 1335
[11] Cao Shao-Chun, Zhang Dong-Ming, Zhang Dian-Lin, Duan H M and Hermann A M 1991 *Phys. Rev.* B **44** 12 571
[12] Cohn J L, Skelton E F, Wolf S A, Liu J Z and Shelton R 1992 *Phys. Rev.* B **45** 13 144
[13] Suleiman B M, Ul-Haq I, Karawacki E, Maqsood A and Gustafsson S E 1993 *Phys. Rev.* B **48** 4095
[14] Bougrine H, Sergeenkov S, Ausloos M and Mehbod M 1993 *Solid State Commun.* **86** 513
[15] Ausloos M and Houssa M 1993 *Physica* C **218** 15
[16] Nuss M C, Mankiewich P M, O'Malley M L, Westerwick E H and Littelwood P B 1991 *Phys. Rev. Lett.* **66** 3305
[17] Bonn D A, Dosanj P, Liang R and Hardy W N 1992 *Phys. Rev. Lett.* **68** 2390
[18] Krekels T, Van Tendeloo G, Broddin D, Amelinckx S, Tanner L, Mehbod M, Vanlathem E and Deltour R 1991 *Physica* C **173** 361
[19] Grandjean I 1993 *Honors Thesis* University of Brussels
Mehbod M, Grandjean I, Schroeder J and Ausloos M 1994 unpublished
[20] Bougrine H, Ausloos M, Houssa M and Mehbod M 1994 *Proc. 4th Int. Conf. on High-T_c Superconductors (Grenoble, 1994)*
[21] Lan M D, Liu J Z and Shelton R N 1991 *Phys. Rev.* B **43** 12 989
[22] Majewski P, Hettich B, Rüffer N and Aldinger F 1993 *Proc. Metallurgical Society of AIME Ann. Meet. (Denver, CO, 1993)*
[23] Bougrine H and Ausloos M unpublished
[24] Ziman J M 1963 *Electrons and Phonons* (Oxford: Clarendon)
[25] Harshmann D R and Mills A P 1992 *Phys. Rev.* B **45** 10 684
[26] Kirichenko Yu A, Kozlov S M, Rusanov K V, Tyurina E G, Titova S G and Fotiev V A 1991 *Superconductivity: Phys. Chem. Technol.* **4** 2256
[27] Kittel C 1986 *Introduction to Solid State Physics* (New York: Wiley)
[28] Yosida K 1958 *Phys. Rev.* **110** 769
[29] Tyley D R and Tyley J 1990 *Superfluidity and Superconductivity* (Bristol: Adam Hilger)
[30] Baber W G and Wills H H 1937 *Proc. R. Soc.* A **158** 383
[31] Ausloos M, Patapis S K and Clippe P 1992 *Physics and Materials Science of High Temperature Superconductors II* ed R Kosowsky, S Metfessel, D Wohlleben and S K Patapis (Dordrecht: Kluwer) p 755
[32] Ausloos M, Laurent C, Patapis S K, Politis C, Luo H L, Godelaine P A, Gillet F, Dang A and Cloots R 1991 *Z. Phys.* B **83** 355
[33] Schneider T and Ariosa D 1992 *Z. Phys.* B **89** 267
[34] Pureur P, Menegotto-Costa R, Rodrigues P, Schaf J and Kunzler J V 1993 *Phys. Rev.* B **47** 11 420
[35] Sergeenkov S 1991 *J. Supercond.* **4** 431
[36] Higashi T, Onuki M, Ishii S, Kubota H and Fujiyoshi T 1991 *Physica* C **185–9** 1357
[37] Fridel B, Thomsen C and Cardona M 1990 *Phys. Rev. Lett.* **65** 915
[38] Sergeenkov S and Ausloos M 1993 *Phys. Rev.* B **48** 4188
[39] Kirichenko A, Kozlov S M, Rusanov K V, Tyurina E G, Titowsa S G and Fotiev V A 1991 *J. Supercond.* **4** 2255
[40] Tewordt L and Wölkhausen Th 1989 *Solid State Commun.* **70** 839
[41] Sergeenkov S, Ausloos M, Bougrine H, Cloots R and Gridin V V 1993 *Phys. Rev.* B **48** 16 680
[42] Bougrine H, Sergeenkov S, Ausloos M, Cloots R and Gridin V V 1994 *Solid State Comm.* at press
[43] Stegmeir E F 1969 *Thermal Conductivity* vol 2, ed R P Tye (London: Academic) p 203